Simulation of an ECT Sensor to Inspect the Reinforcement of Concrete Structures

Naasson P. de Alcantara Jr.*, Luiz Gonçalves Jr.
São Paulo State University – Unesp. Department of Electrical Engineering
*Av. Luiz E. C. Coube, 14-03, Bauru,SP, Brazil. naasson@feb.unesp.br

Abstract: This paper describes the use of COMSOL Multiphysics to simulate an ECT (Eddy Current Testing) sensor, designed to inspect the elements of the reinforcement of concrete structures. The electromagnetic parts of the sensor constitute a RLC series circuit, where L is the inductance of a multi-turn coil, R is the total resistance, (the coil resistance and an external one), and C is an external capacitance. The paper describes the steps for the COMSOL simulation. Simulations were done for three configurations of the sensor, and the results will be presented graphically.

Keywords: Concrete structures, Non-destructive evaluation, Eddy current testing, Finite element method, COMSOL Multiphysics.

1. Introduction

Due to its high plasticity, high load-carrying capacity and low-maintenance requirements, rebar-reinforced concrete is used in almost all civil structures including commercial, industrial and residential buildings, dams, power plants, bridges, stadiums etc. Its high strength, durability, sustainability and flexibility allow to produce the most complex shapes of concrete structures. However, although reinforced concrete is a relatively durable and robust constructional material, its performance can decline dramatically over time. When exposed to adverse physio-chemical environmental conditions may lead to premature loss of strength due to corrosion of rebar. These defects can result in catastrophic structural failure unless their presence is detected and their effects are assessed in time. To keep a high level of structural safety, durability and performance of concrete structures, efficient systems for early and regular structural assessment is mandatory. The quality assurance during and after the construction of new structures, after reconstruction processes, as well as the characterization of material properties and damage as a function of time and environmental influences, is a serious concern.

As a contribution to the theme, this paper focuses on the use of eddy current NDT techniques to inspect the reinforcement of concrete structures.

Eddy current methods can be used to analyze conductive materials through electromagnetic induction. The probe device itself is nothing more than an AC transformer. Eddy Current probes work based on the following basic electromagnetic concepts: 1) Current flow in a coil generates a magnetic field. 2) A magnetic field in proximity to a conductor produces an electromotive force (in Volts), in the conductor. If the conductor is a closed circuit, a current (in Amperes) will flow. This current will produce an opposite magnetic field that will react against the variation of the original magnetic field. In the case of solid conductor materials, eddy current loops will appear within it. Eddy current measurement consists of five steps: 1) Signal excitation. 2) Material interaction. 3) Signal pickup. 4) Signal conditioning and display. 4) Analysis.

The use ECT in the identification of the reinforcement of concrete structures has been present in the related literature [1], [2], [3]. In a previous paper [4], the first author of the present paper built differential electromagnetic sensors, produced dozens of reinforced concrete samples, and performed laboratory tests. The results were used to construct ANN training vectors, in order to locate and identify steel bars under the concrete cover.

In this paper, COMSOL Multiphysics [5] will be used to simulate a new kind of ECT sensor, designed to inspect the elements of the reinforcement of concrete structures. The sensor is, basically, a RLC series circuit, whose basic principles will be described in the next section.

2. Description and Mathematical Basics of the Proposed ECT Sensor

The sensors proposed in this work are, basically, RLC circuits, where L is the inductance of a multi-turn coil, Lc, R is the sum of the coil resistance Rc and any other additional

resistance, Re, and C is the capacitance of an external capacitor, Ce, connected in series with the coil. Figure 2 shows an equivalent electrical circuit of the sensor.

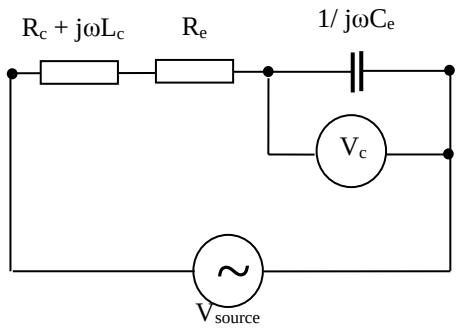

Figure 1. An electrical circuit of the ECT sensor for reinforcement inspections.

V_{source} is the voltage applied at the terminals of the sensor, and V_c is the voltage measured across the capacitor terminals. Using the Kirchoff's second law, V_{source} and V_c can be expressed as:

$$V_{source} = Ri + j\omega Li - j\frac{1}{\omega C}i \qquad (1)$$

and

$$V_c = -j\frac{1}{\omega C}i \qquad (2)$$

where $R = R_e + R_c$, and the indexes are suppressed. Expliciting the current in equation (1), substituting in equation (2), and developing algebraically, the voltage at the terminals of the capacitor can be expressed as:

$$V_c = -V_{source}\frac{(\omega^2 CL - 1 + j\omega CR}{(\omega CR)^2 + (\omega^2 CL - 1} \qquad (3)$$

At the resonant frequency, $\omega L = 1/(\omega C)$, and equation (3) is drastically reduced.

3. Use of COMSOL Multiphysics

3.1 Constructing the Model

A 3D model was developed, using COMSOL Multiphysics. The first step was to define Magnetic Field and Electrical Circuit as the physics of the problem, and frequency domain for the type of solution.

The next step was to model the ECT sensor. A multi-turn coil, a ferrite box surrounding the coil, and an aluminum box, to provide the external shielding for the sensor, will constitute it. Figure 2 shows, in a exploited way, the components of the sensor.

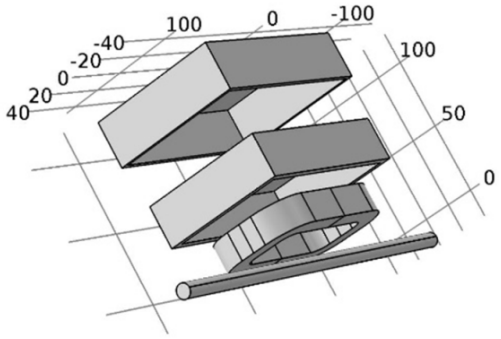

Figure 2. The elements of the ECT sensor. From bottom to top: the steel bar, multi-turn coil, ferrite box and aluminum box.

These components were defined using the options of the *Geometry tool bar* of COMSOL. Using the Explicit option of the *Definition tool bar*, the dominions were assigned as: Steel bar, Coil, Ferrite box, Shielding and Air. After, the materials were defined using the built in material library (Air, structural steel, Ferrite and Aluminum), and the characteristics of the multi-turn coil was set (Coil type: Numeric, Coil excitation: current, Number of turns: 800, coil conductivity 5.8×10^7 S/m, and 24 AWG). As the Magnetic Field physics interface was used, Ampere's Law and Initial Values conditions were naturally imposed. Finally, magnetic Insulation was applied to the boundaries of the coil.

Meshing was chosen according to the regions of interest, using predefined size options. Coarse to the air up to extra fine, to the shielding. Free tetrahedral elements were used. No special features, like sweep and boundary layers were necessary. Figure 3 shows the generated mesh, hiding the air discretization.

3.2 Running COMSOL to Compare the Magnetic Flux Behavior for Some Sensor Configurations

After to establish the model, the simulation was done. Three configurations were considered for the sensor:

1. The sensor is built using only the coil, without the ferrite box and the aluminum shielding.
2. The sensor is built using the coil and the ferrite box, but without the aluminum shielding.
3. The sensor is built in its complete configuration (all the elements are present: the coil, the ferrite box and the aluminum shielding).

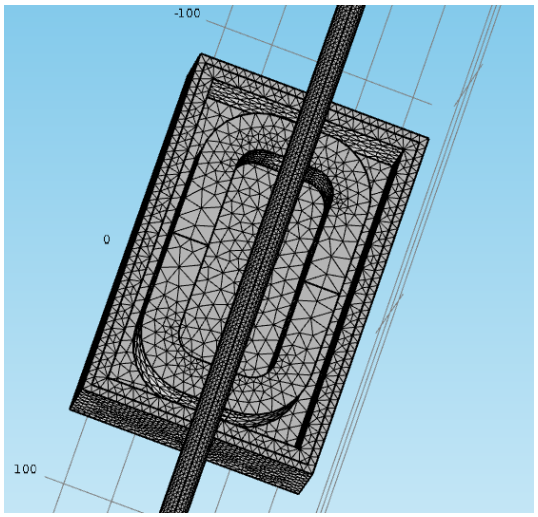

Figure 3. Generated mesh for the model.

Before to start the simulations with the presence of the steel bar under the sensor, initial simulations were done in order to calculate the inductance of the coil in each case. The presence of materials like ferrite and aluminum in the sensor affects significantly the resultant inductance of the coil, and the use of the COMSOL allows the calculation of this parameter with a high level of reality. The results for these initial simulations are summarized in table 1.

Table 1: Inductances of the sensor at no-load

	frequency	inductance
Case 1	8.15 kHz	70.65 mH
Case 2	7.00 kHz	102.43 mH
Case 3	7.00 kHz	90.92 mH

In all three cases, a source voltage of 3.53 V_{rms} (10 V_{pp}) was considered. This value is not relevant because the inductance is not dependent on the level of excitation in cases such as these. The magnetic materials present in the system will never work close to their saturation levels.

Case 1: Figures 4 and 5 shows the magnetic flux density norm at the surfaces of the coil and the steel bar, when it is positioned at 20 mm bellow the center of the sensor, as well in regions where would be placed the ferrite box.

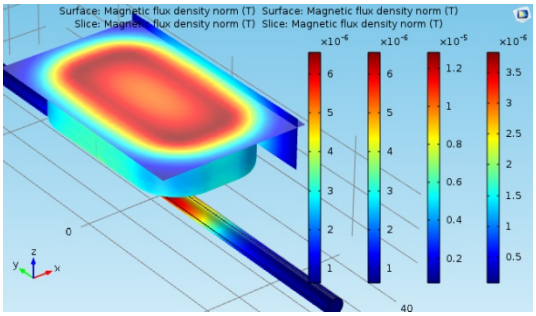

Figure 4. Magnetic flux density at the coil and steel bar surfaces, and within regions that would be occupied by the surrounding ferrite box (top perspective), Legends, from left to right: ferrite box regions (twice), coil and steel bar.

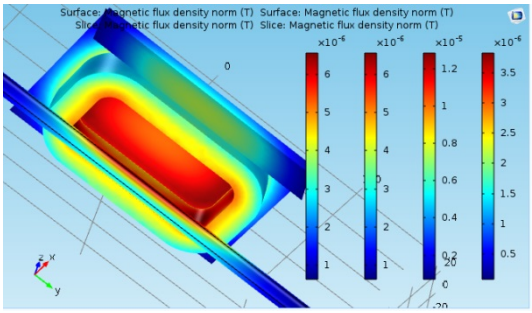

Figure 5. Magnetic flux density at the coil and steel bar surfaces and within regions that would be occupied by the surrounding ferrite box (bottom perspective). Legends are the same as figure 4

Figures 6 and 7 show details of the eddy current induced within the steel bar.

The important information that can be obtained from these graphics is the following. 1) The values of magnetic induction in the materials are very low, ensuring that the sensor will always operate in the linear region, with respect to the magnetic field. 2) Eddy current will be

induced in the bar portion that is right under the sensor, and it is important in order to decide which will be the size of its coverage upon the bar.

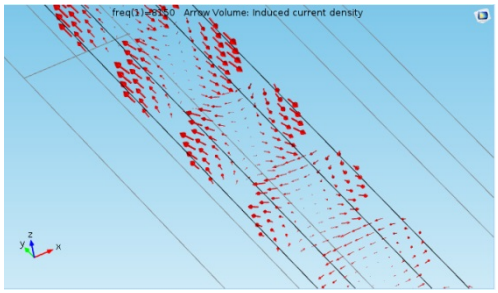

Figure 6. Eddy current induced within the steel bar.

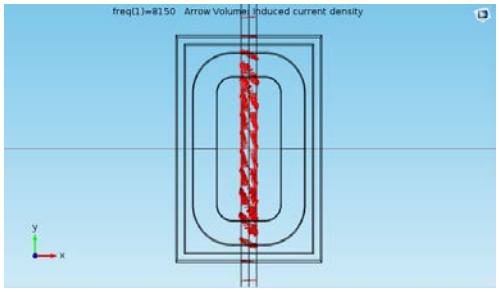

Figure 7. Eddy current induced within the steel bar.

Case 2: Figures 8 and 9 shows the magnetic flux density norm at the surfaces of the coil and the steel bar, and within the walls of the ferrite box.

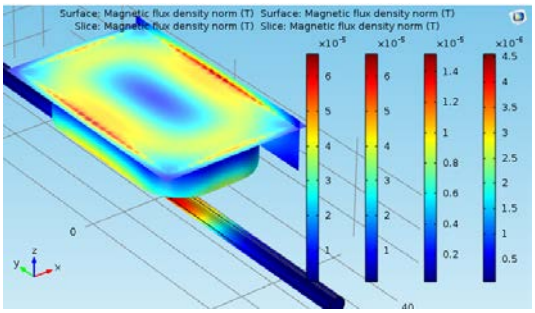

Figure 8. Magnetic flux density at the coil and steel bar surfaces, and within the walls of the ferrite box (perspective from the top). Legends, from left to right: ferrite upper wall and right wall, coil and steel bar.

Comparing figures 4 and 8 is possible to conclude that the maximum value of magnetic flux density at the steel bar is increased about 28% in relation to the case 1. This conclusion is very important, because the higher the flux density, the greater will be the amount of energy transferred to the bar, and therefore greater signal variations can be observed. In addition, the presence of the ferrite box surrounding the coil causes an increasing by a factor of ten in the magnetic field density in the region close to the winding. In other words, again is possible to see a better coupling between the magnetic flux and the steel bar.

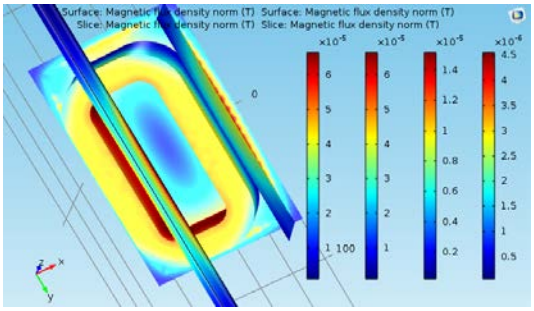

Figure 9. Magnetic flux density at the coil and steel bar surfaces, and within the walls of the ferrite box (perspective from the bottom). Legends, from left to right: ferrite upper wall and right wall, coil and steel bar.

Case 3: Figure 10 shows the magnetic flux density norm at the surfaces of the coil and the steel bar, and within the walls of the aluminum box.

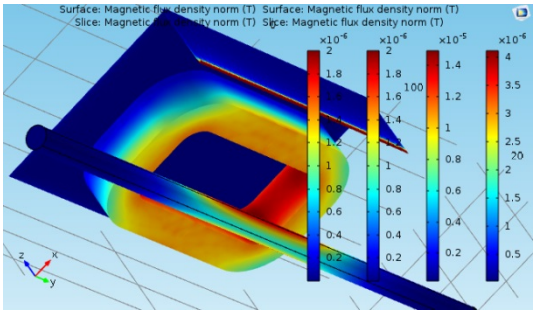

Figure 10. Magnetic flux density at the coil and steel bar surfaces, and within the walls of the aluminum box (perspective from the bottom). Legends, from left to right: aluminum upper wall and right wall, coil and steel bar.

In this case, it is easy to see that the magnetic flux density within the aluminum box is very close to zero. The ferrite box only is sufficient to act as a shielding for the sensor.

3.3 Running COMSOL to Simulate the Sensor Movement over the Steel Bar

COMSOL Multiphysics was used to simulate the sensor movement over the steel bar, for the

three configurations presented in the previous subsection. Figure 11 represents the position of the steel bar in relation to the sensor.

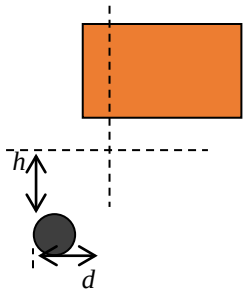

Figure 11. Schematic representation of the sensor position in relation to the steel bar.

In figure 11, *h* is the distance between the top of the bar and the base of the sensor and *d* is the distance between the center of the bar and the axis of the sensor.

The gauge of the steel bar used in the simulation is 10 mm. Six values for the horizontal displacement (*d* = 100, 80, 60, 40, 20 and 0 mm), and two values for vertical position (*h* = 10 and 20 mm) were considered. Figure 12 shows the results.

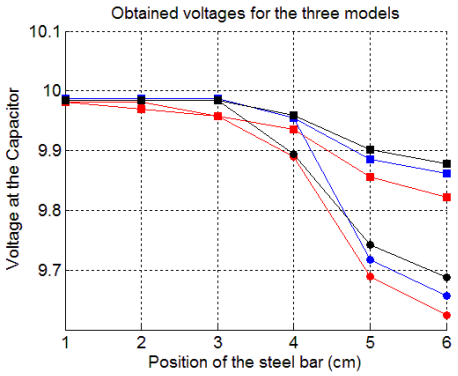

Figure 11. Obtained results for the three sensor configurations, in function of the position of the sensor.

In figure 12, black curves are the results for the case 1 simulation; red curves are the results for case 2 and blue curves the results for case 2. Red marks are the results for *h* = 10 mm and circle marks the results for *h* = 20 mm. The input voltage was set to produce approximately 10 V in each sensor configuration, at no load condition.

The best results are those for the case 2 configuration, and agree with the observations made for the results presented in the previous subsection.

4. Conclusions

This paper described the use of COMSOL Multiphysics to model the electromagnetic parts of an ECT sensor, designed to inspect the armature elements of reinforced concrete structure. Three models for the sensor were proposed, and analyzed, based on finite element simulations, with regard to their electromagnetic behavior. The performance of the sensors were also simulated and the results were satisfactory in all the cases, but with advantages for the configuration discussed in the case 2 (The use of a ferrite box surrounding the sensor coil, but without an external aluminum shielding). COMSOL Multiphysics proved to be very useful in the three-dimensional modeling of electromagnetic components of this type of application, and the results are very encouraging for future works.

5. References

1. Yokota, O., Study of Reinforcing Bars Detection Buried in Concrete Structures Using Eddy Current Method, in: *15th WCNDT-World Congress on Non-destructive Testin*, (2000), available online www.ndt.net/article/wcndt00/, (accessed on 31/08/2015)

2. Pudov, V., Electromagnetic Devices for the assessment of the State of Reinforcement Elements in Reinforced Concrete Structures, *Russian J. of Non-destructive Testing*, **42**, 26-37 (2006)

3. Rubinacci, G., Tamburino, A., Ventre, S., *Int. J. of Applied Electromagnetic and Mechanics*, **25**, 333-339, (2005)

4. Alcantara Jr., N. P, Identification of Steel Bars Immersed in Reinforced Concrete Based on Experimental Results of Eddy Current Testing and Artificial Neural Network Analysis, *Nondestructive Testing and Evaluation*, **28**, 58-71 (2013)

5. *COMSOL Multiphysis*, Avaliable online, http://comsol.com, (accessed on 20/09/2015).

6. Acknowledgments

The authors express their gratitude to the FAPESP – São Paulo Research Foundation, for the financial support of this research, under the grants number 2014/08797-8.